EARTH SCIENCES
RESEARCH JOURNAL
Earth Sci. Res. J. Vol. 29, No. 3 (September, 2025):287 - 296

UNIVERSIDAD NACIONAL DE COLOMBIA

MINERALOGY

Chemical characterization and valorization potential of subsurface gypsum deposits in the Boufatis Plateau, Lower Chelif Basin (NW Algeria)

Abdelkader Boucif[1,2]*; Matthias Reimann[3,4]; Mustapha Bensalah[1]; Hakim Hebib[1,2]; Ali Kacemi[1,2];
1. Department of Earth and Universe Sciences, University of Tlemcen, P.O. Box 119, Tlemcen 13000, Algeria.
2. Laboratory: Promotion of Water, Mineral and Soil Resources, Environmental Legislation and Technological Choices
3. Knauf Gips KG, Germany.
4. University of Würzburg, Institute of Geography and Geology, Geography Building Am Hubland 97074 Wuerzburg, Germany.
* Corresponding author: abdelkader.boucif@univ-tlemcen.dz

ABSTRACT

Gypsum represents a major strategic resource, widely used in plaster production and its derivatives, serving as a fundamental construction material. Given its important role in the industry, it is imperative to ensure efficient and sustainable management of this raw material in order to meet growing market demands while preserving natural resources. This study is based on data obtained from core drilling conducted in Djebel Djira, located 24 km southeast of Oran. 425 gypsum samples were collected, including 413 for chemical analysis, 10 for physical tests, and 2 for a mineralogical study. This study provides, for the first time, a comprehensive characterization of the chemical and lithological properties of gypsum, offering critical insights into its potential valorization. The analyses reveal that the main oxides are CaO (33.46%) and SO_3 (43.58%), meeting the standards for plaster production. The MgO (0.30%) and K_2O (0.07%), remain within the limits in compliance with industrial requirements. The average chloride content (0.011%) and the low Na_2O concentration (0.09%) promote the setting time of the plaster. These results classify the gypsum in category I according to ISO 1587 certification and the European standard NF EN 520 +A1. 3D models generated using Rockworks software indicate that the eastern and southeastern regions of Djebel Djira are characterized by a minimal overburden, not exceeding 10 meters, whereas gypsum deposits are well developed at greater depths. It is recommended to prioritize the extraction activities in the eastern part of the deposit or in its south-eastern section. In contrast, the western portion of the site should be avoided during early mining works. In this area, the overburden is particularly thick. Gypsum is generally reached only at an average depth of 50 meters, which significantly complicates exploitation operations and increases extraction costs.

Keywords: Gypsum; Chemical analysis; Construction material; Valorization potential; Sustainable management.

Caracterización química y potencial de valorización de los depósitos subterráneos de yeso en el altiplano de Boufatis, cuenca baja de Chelif, noroeste de Argelia

RESUMEN

El yeso representa un recurso estratégico principal, al ser un material fundamental de construcción que se usa ampliamente en la producción de revestimientos y sus derivados. Dado su importante papel en la industria, es necesario asegurar la administración eficiente y sostenible de esta materia prima para alcanzar la creciente demanda del mercado, al tiempo que se preservan los recursos naturales. Este estudio se basa en la información obtenida de perforaciones realizadas en Djebel Djira, ubicada a 24 kilómetros al sureste de Oran (Argelia). Se recolectaron cuatrocientos veinticinco muestras de yeso, de las cuales 413 fueron sometidas a análisis químicos, diez a pruebas físicas, y dos a estudios mineralógicos. Este estudio presenta, por primera vez, una caracterización completa de las propiedades químicas y litológicas de yeso, y ofrece información determinante sobre su potencial de valorización. Los análisis revelan que los óxidos principales son CaO (33,46%) y SO_3 (43,58%), cumpliendo con los estándares para la producción de yeso. El MgO (0,30%) y K_2O (0,07%) permanecen dentro de los límites de conformidad con los requisitos industriales. El contenido medio de cloruro (0,011%) y la baja concentración de Na_2O (0,09%) promueven el tiempo de fraguado del yeso. Estos resultados clasifican el yeso como categoría I según la certificación ISO 1587 y la norma europea NF EN 520 + A1. Los modelos 3D generados utilizando el software Rockworks indican que las regiones oriental y sudoriental de Djebel Djira se caracterizan por una sobrecarga mínima, que no supera los 10 metros de profundidad. Por el contrario, los depósitos de yeso están bien desarrollados a mayores profundidades. Se recomienda priorizar las actividades de extracción en la parte oriental del depósito o en su sección sudoriental. En cambio, la parte occidental del yacimiento debe evitarse durante las primeras labores mineras. En esta zona, la sobrecarga es especialmente gruesa. El yeso generalmente solo se alcanza a una profundidad promedio de 50 metros, lo que complica considerablemente las operaciones de explotación y aumenta los costos de extracción.

Palabras clave: yeso; análisis químico; material de construcción; potencial de valorización; manejo sostenible.

Record
Manuscript received: 11/01/2025
Accepted for publication: 20/08/2025

How to cite this item:
Boucif, A., Reimann, M., Bensalah, M., Hebib, H., & Kacemi, A. (2025). Chemical characterization and valorization potential of subsurface gypsum deposits in the Boufatis Plateau, Lower Chelif Basin (NW Algeria). *Earth Sciences Research Journal, 29*(3), 287-296. https://doi.org/10.15446/esrj.v29n3.118266

ISSN 1794-6190 e-ISSN 2339-3459

https://doi.org/10.15446/esrj.v29n3.118266

1. Introduction

Gypsum is widely used in the manufacture of plaster and its derivatives, which constitute fundamental materials in the construction industry. In addition to their structural role, these materials provide effective thermal and acoustic insulation, contributing significantly to building comfort. The present study forms part of a broader geological exploration program initiated through a collaboration between the German company Knauf Gips KG and the Center for Technological Studies and Services in the Construction Materials Industry (CETIM). The gypsum deposits observed in the Djebel Djira region are closely linked to the Messinian Salinity Crisis (MSC), a significant geological event that occurred between approximately 5.97 and 5.33 million years ago (Roveri et al., 2014; Lanzoni, 2022; Krijgsman et al., 2024). This crisis has resulted in the partial or complete isolation of the Mediterranean Sea of the Atlantic Ocean, most likely due to tectonic or glacio-eustatic processes (Pérez-Asensio et al., 2013; Krijgsman et al., 2024). As a result, substantial gypsum layers accumulated in the peripheral basins of the Mediterranean, generally at depths not exceeding 200 m (Sellam et al., 2025). This context led to the formation of the Lower Primary Gypsum unit (PLG), with thicknesses reaching up to 300 m (Stefano et al., 2010; Lugli et al., 2010; Caruso et al., 2015; Bigi et al., 2024). All Neogene formations were thoroughly investigated due to their abundant surface exposures. In contrast, gypsum deposits rarely outcrop, significantly limiting data collection opportunities and, in the current state of knowledge, few works have dealt with this subject (Remmache, 2006; Alouasi et al., 2022; Sellam et al., 2025). This lack of data poses a major challenge because it limits our knowledge of the lithological and chemical properties of gypsum, thus hampering efforts to optimize its industrial application.

In this study, as part of a geological exploration campaign, core-drilling work was initiated. The objective was not only to determine the strength and quality of the gypsum beds but also to study the lithological nature and thickness of the barren layers unsuitable for exploitation. In total, 35 vertical mechanical boreholes were drilled, with a combined length of 1,686 meters. The recovered cores were described onsite, organized, and classified for each borehole. The collected gypsum samples were sent to the Center for Studies and Technological Services of the Construction Materials Industry (CETIM) for physicochemical analyses. Surfer software (version 18) was used to create facies maps and assess geological reserves. RockWorks 17 software was employed to develop a database for generating two- and three-dimensional geological models and profiles. These simulations allow for a more efficient design of the structure, the geometry of the gypsum bed, and the cover depth. As a result, they support optimal and cost-effective planning during exploitation activities.

2. Geological setting

2.1 Lower Chelif Basin

The Lower Chelif Basin has been the subject of several studies since the first geological reconnaissance studies by Bleicher (1875), Pomel (1892), Repelin (1895), and Brives (1897), up to the eminent works of the National Society for Oil Research and Exploitation in Algeria, the S.N. Repal Company (1952), Dalloni (1952), Perrodon (1957), Gourinard (1958), Delteil (1974), Fenet (1975), Guardia (1975), Rouchy (1982), Thomas (1985), and Neurdin-Trescartes (1992, 1995). Other more recent works on stratigraphic, paleontological, and micropaleontological levels were initiated in the 1990s (Belkebir et al., 1994, 1996, 2002, 2008; Rouchy et al., 2007; Atif et al., 2008; Belhadji et al., 2008; Mansouri et al., 2008; Satour et al., 2013; Hebib, 2014; Benzina et al., 2019; Belhadji, 2021; Moulana et al., 2021; Khalili et al., 2022; Atik et al., 2024; Bouchemla et al., 2025). The Lower Chelif Basin is a subsiding, intramontane, and synorogenic basin linked to the paroxysmal phases of Alpine orogeny (Perrodon, 1957; Thomas, 1985). It corresponds to the median furrow (Delfaud, et al., 1973), surrounded by two longitudinal depressed zones, the Murdjadjo-Arzew-Dahra massifs to the north and the Tessala-Ouled Ali-Beni Chougrane-Ouarsenis Mountains to the south (Fig.1).

The lower Chelif Basin appears as a NE-SW trending depression that is 300 km long and 80 km wide. It consists of a Tertiary-age terrain. The Miocene deposits are predominant, with thicknesses approaching 4000 m at the basin center and decreasing considerably toward the margins (S.N. Repal 1952; Perrodon, 1957; Bessedik & Belkebir, 1985). The upper Miocene is represented by blue marls of the Tortonian age that begin with well-developed sandstones on the margins passing to diatomites or marls with diatomitic intercalations of the Messinian age. At the Messinian end, the facies evolved toward essentially gypsiferous evaporitic sedimentation (Rouchy, et al., 1981; Neurdin-Trescartes, 1995). A coral edifice has developed on platform margins and basin highs (Saint Martin, 1987 ; Saint Martin & André, 1992). The Pliocene generally begins with white marls passing locally to alternations of marl and sandstone (Benyoucef et al., 2021).

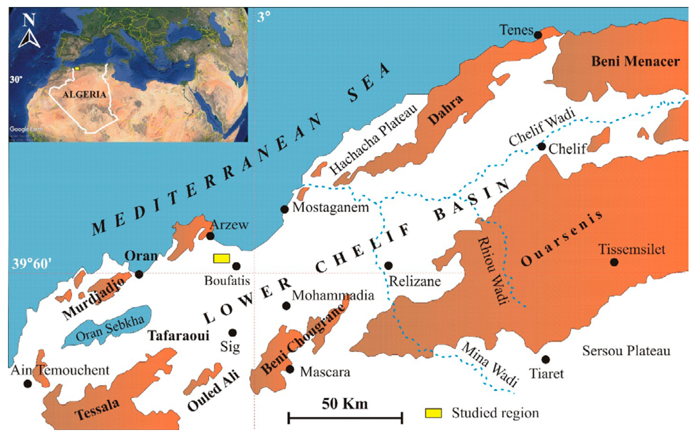

Figure 1. Location map of the Lower Chelif basin and the main mountain ranges (NW Algeria)

2.2 Boufatis Plateau

The Boufatis Plateau occupies the western part of the Lower Chelif Basin, consisting mainly of Mio-Plio-Quaternary terrains (Perrodon, 1957) resting unconformably on the Secondary-age Arzew massifs. Structurally, the Boufatis Plateau consists of a succession of anticlines and synclines aligned in a northeast-southwest direction (Fig. 2).

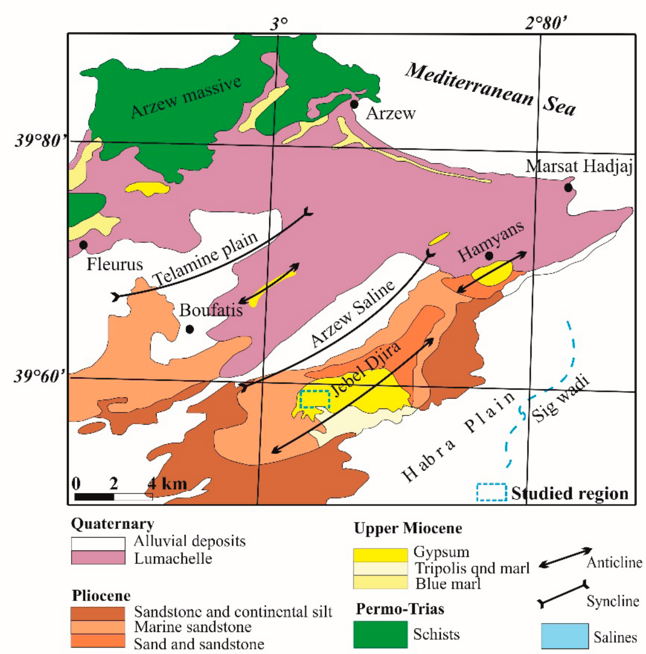

Figure 2. Geological map of major units in Northwestern Algeria (St. Cloud map, N°154, 1:500,000)

The Miocene and Pliocene terrains constitute the largest part of the Lower Chelif Basin, with a thickness of approximately 4,000 m in axial zones, decreasing considerably towards the margins (Belkebir et al., 2008). The Miocene series is divided into two sedimentary cycles: a Lower Miocene cycle corresponding to a time interval from the upper Burdigalian to the terminal Serravallian (Moussa, et al., 1994; Bessedik et al., 2002), and an Upper Miocene cycle encompassing the Tortonian and Messinian stages (Belkebir, et al., 2008). Blue marls of Tortonian age, typically beginning with well-developed sandstone layers on the margins that transition into diatomites or marls with diatomitic intercalations characterize the Upper Miocene (Perrodon, 1957; Rouchy, 1990; Benzina et al., 2019). The Messinian deposits then evolve towards an evaporitic sedimentation that is essentially gypsiferous (Bertoni, 2015). Discordant with preceding formations, the Pliocene is commonly represented by white marl, locally evolving into marl with sandstone layers. The Pleistocene is marked by hard, yellowish-brown limestones forming a surface crust, along with gray-yellow lumachelic limestones that are well exposed throughout the region. Finally, the Holocene consists of saline deposits in Sebkhas and valleys, typically devoid of vegetation (Fig. 3).

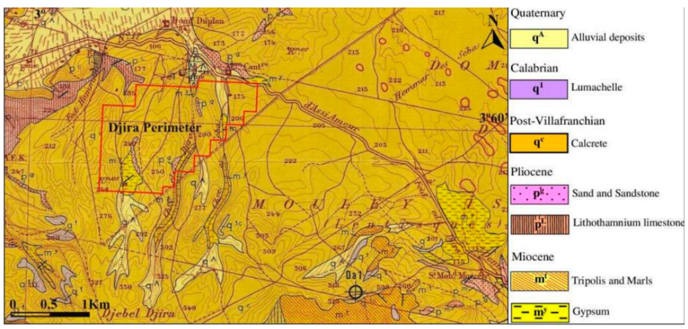

Figure 3. Geological map of studied region, showing the upper Miocene (Gypsum deposits, m^y), the Pliocene and the Quaternary lithostratigraphic succession.

3. Materials and methods

The Djebel Djira deposit is composed of four hills separated by wadis. It displays a relatively regular structure with a gentle dip and an almost flat relief. For the borehole distribution network, a grid spacing of 200 × 300 m was applied in the eastern part of the deposit, while a wider spacing of 400 × 500 m was used in the western part. In total, 35 vertical mechanical boreholes were drilled, representing a cumulative depth of 1686 m. Drilling was carried out using a double-core barrel system (wireline) to minimize sample disturbance and to ensure optimal preservation of the cores. Boreholes had a diameter of 45 mm. When clear water was employed as the drilling fluid, injection was performed between the two tubes, preventing direct contact of the core with the rotating barrel. The recovered cores were systematically logged for detailed geological documentation. The boreholes are distributed along ten parallel profiles NNW–SSE oriented (Fig. 4). Boreholes located between profiles I and VII reached an elevation of +140 m and successfully intersected the gypsum bed. In contrast, boreholes 1, 3, 13, 14, and 15, positioned between profiles VIII and IX, did not attain this elevation and intersected the gypsum bed with a thickness ranging from 3 to 6 m. These boreholes were primarily designed to assess the thickness of the overlying cover. Boreholes 2 and 17 were drilled to depths exceeding 40 m without intersecting the gypsum bed. Overall, the core recovery rate was greater than 90% within the gypsum layers, but decreased significantly in friable, unstable, or heterogeneous lithologies such as sandstone.

X-ray diffraction (XRD) was used to determine the oxide content of gypsum from Djebel Djira. Generally, this technique involves projecting an X-ray beam onto a crystal, which is deflected by the atomic planes of the crystal lattice, producing a unique signature specific to each mineral. Gypsum samples are ground to a powder with a particle size of less than 2 mm (Janssens, 2004). This approach enabled us to accurately identify the oxide content and estimate their relative proportions in the gypsum studied.

In order to process all this data, we created a database under RockWorks. The latter is a powerful software dedicated to various geoscience sectors, designed for processing, modeling and visualizing subsurface data, particularly core and drilling data. It uses geological, geochemical and geotechnical data in 2D/3D models, making it essential for mining, hydrogeological and civil engineering projects.

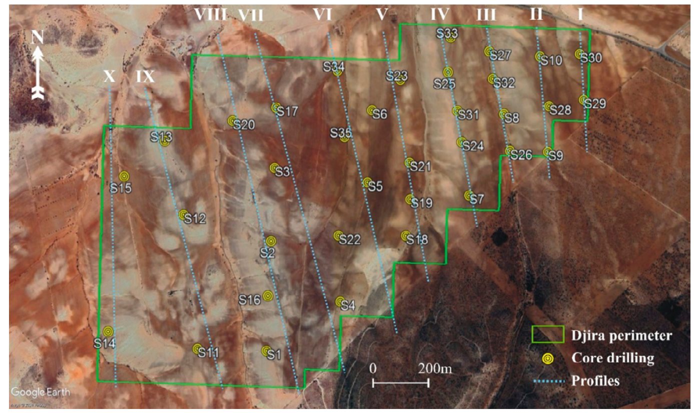

Figure 4. Satellite imagery of Djebel Djira delineating the study perimeter and locations of core drilling along 10 profiles.

4. Results and discussion

4.1 Core drilling data

The gypsum layers are largely concealed beneath Quaternary alluvial deposits composed of medium-hard calcareous crusts, yellowish clays, and lumachelic limestones. The thickness of the overburden increases progressively from approximately 5 m in the East to more than 40 m in the West. The isobath map shows that the eastern sector of the deposit is generally characterized by a thinner cover, ranging from 5 m to 23 m, with the exception of borehole 20 where the overburden exceeds 30 m (Fig. 5).

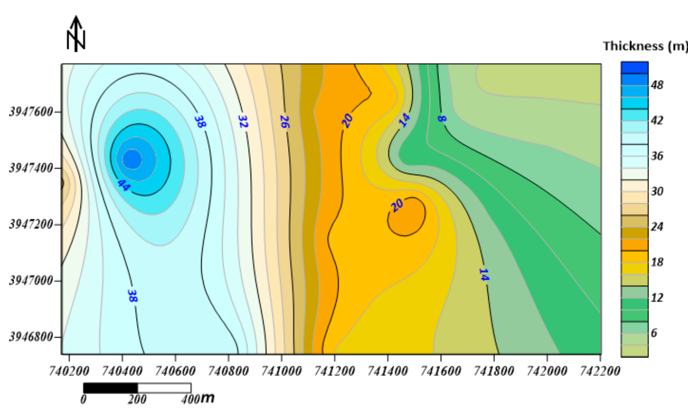

Figure 5. Isobath map of overburden thickness variation in the Djebel Djira deposit.

The central part of the deposit is characterized by cover thicknesses ranging between 15 m and 30 m. In contrast, the western sector shows a markedly thicker overburden, exceeding 40 m. Concerning the exploitable bed, gypsum outcrops are observed in the eastern part of the deposit, where thicknesses vary between 15 m and more than 50 m, with an average of approximately 35 m. Notably, the thickness of the gypsum bed decreases westward, while the thickness of the overlying cover increases (Fig. 6).

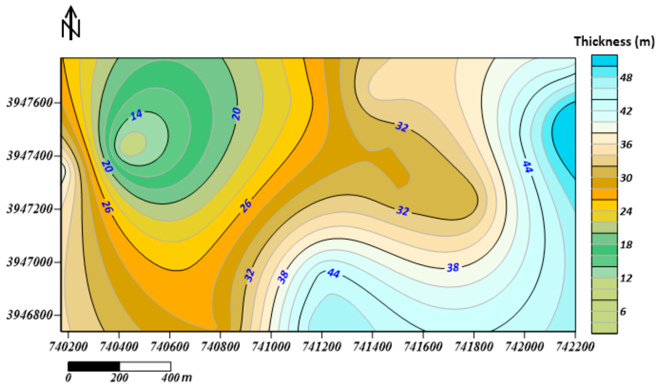

Figure 6. Isopach map showing the variation in thickness of the gypsum layer in the Djebel Djira.

This finding will guide future exploitation efforts, suggesting that rock extraction should begin in the eastern or southeastern part of the deposit (Fig. 7). For optimal extraction planning, beyond the volume of reserves, it is essential to consider several key parameters, including site accessibility, the structural characteristics of the deposit, local topography, and environmental impacts. Previous studies have emphasized the importance of integrating such multidisciplinary datasets in mining planning and sustainable exploitation (Zhang et al., 2020; McQuillan, & Bar, 2023). Data such as access route mapping, 3D models of the deposit (derived from drilling and geophysical surveys), the mechanical properties of the rocks, and a detailed digital terrain model, will allow for the assessment of slope stability and geotechnical constraints, as demonstrated in comparative works on gypsum and evaporite deposits (Zheng et al., 2019). Furthermore, an environmental analysis including the mapping of sensitive ecosystems, hydrological risks, and potential dust or noise emissions is indispensable for sustainable exploitation, in line with recommendations from regional and global case studies (Boukria et al., 2022). The integration of these data, obtained through remote sensing (Lidar, drones), core sampling, laboratory tests, and numerical simulations, will ensure informed decision-making, minimizing both operational risks and ecological impact.

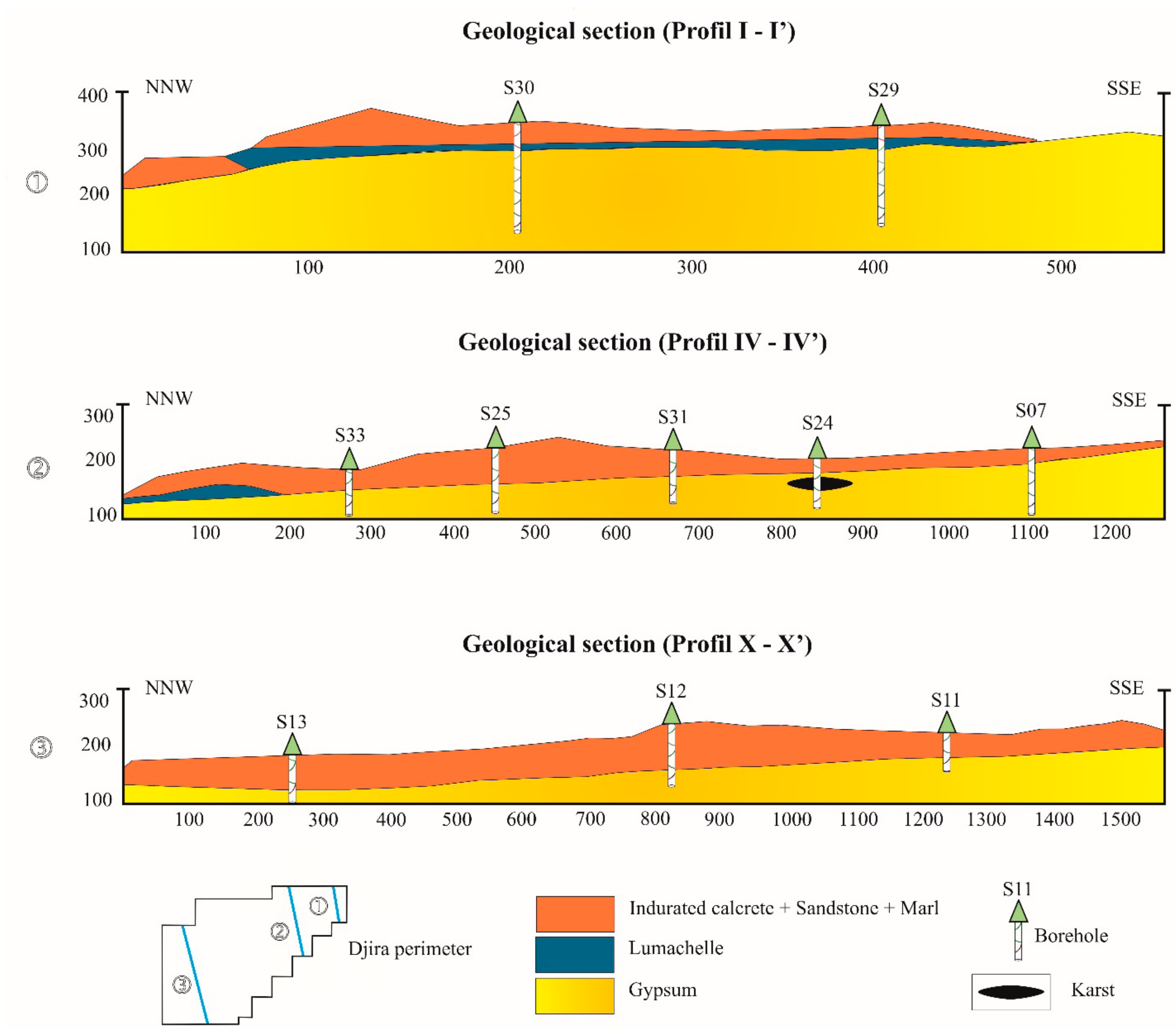

Figure 7. Geological sections and stratigraphic correlations according to profiles of Djebel Djira

In order to evaluate the quality of the rock mass through parameters such as fracturing, cohesion, and compactness, we present as an illustration the results from borehole N° 22, along with the percentage obtained from analysis of the RQD (Rock Quality Designation) index. This approach enables interpretation of the rock mass quality and prediction of its mechanical behavior during extraction operations (Shen, et al., 2023 ; Yu, et al., 2024). This RQD concept, introduced by Deere in 1964, makes it possible to evaluate the mechanical quality of a rock mass based on geological cores (Chalhoub, 2006; Armatys, 2012). This quantitative index corresponds to the ratio (expressed as a percentage) between the cumulative length of intact core fragments (longer than 10 cm) and the total length of the drilled section. The methodology relies on a selective approach: only cohesive fragments of significant size are considered in the calculation, thus excluding fractured or altered zones. This parameter is expressed by the following equation (1):

$$RQD\ (\%) = \left(\frac{\sum \text{Lengths of intact core pieces} \geq 10\ cm}{Total\ drill\ run\ lengths}\right) * 100 \qquad (1)$$

The correlation between the RQD index and the quality of the rock mass is based on the classification proposed by Deere (1968), presented in Table 1 below.

Table 1. Relationship between RQD values and rock mass quality grades (Deere, 1968)

RQD	Rock mass quality
< 25%	Very poor rock
25–50%	Poor
50–75%	Fair
75–90%	Good
90–100%	Excellent

For borehole N°22, the calculated average RQD values range between 65% and 100%. According to the classification proposed by Deere (1968), these values indicate a rock mass quality ranging from good (RQD between 75–90%) to excellent (RQD > 90%). This distribution suggests that the rock mass encountered in this borehole exhibits a generally coherent structure with a low degree of fracturing, reflecting favourable mechanical stability conditions for exploitation (Fig. 8).

KNAUF Plâtres Fleurus

Djebel Djira : Bore hole N°22	
X	740 891
Y	3 946 740
Z	217 m

From (m)	To (m)	Recovery	RQD	Description
0,00	2,50	44%	55%	Red clay interspersed with angular to subrounded clasts of beige sandstone of centimetric grain size (2-8 cm).
2,50	5,50	40%	65%	
5,50	7,00	48%	40%	
7,00	8,50	20%	15%	Intercalations of decimetric beds of friable sandstone (fine to medium grain) and whitish limestone, with a remarkable level sandstone with bivalve debris.
8,50	10,00	20%	25%	
10,00	11,50	35%	20%	
11,50	14,50	0%	30%	
14,50	17,50	65%	45%	Gypsum appears at a depth of 16 m, gray in color, with large crystals that are sometimes fragmented, and a brown clayey joint between the crystals.
17,50	20,50	70%	78%	
20,50	23,50	100%	85%	Whitish gypsum exhibiting large spearhead-shaped crystals.
23,50	26,50	100%	97%	
26,50	29,50	95%	95%	Greenish marl containing gypsum crystal inclusions. The gypsum is grayish and macrocrystalline.
29,50	32,50	100%	100%	
32,50	35,50	85%	100%	
35,50	38,50	100%	100%	
38,50	41,50	80%	90%	Green plastic marl.
41,50	44,50	100%	95%	Gray macrocrystalline gypsum.
44,50	47,50	100%	100%	
47,50	50,50	95%	95%	
50,50	53,50	75%	65%	Green plastic marl.
53,50	56,50	88%	77%	Gray macrocrystalline gypsum.
56,50	59,50	95%	92%	
59,50	62,50	100%	100%	
62,50	65,50	100%	100%	
65,50	68,50	98%	100%	
68,50	71,50	90%	85%	
71,50	74,50	85%	75%	
74,50	77,50	100%	90%	Gray macrocrystalline gypsum.
77,50	80,50	100%	95%	

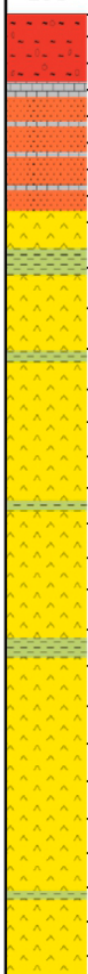

Pictures

Figure 8. Lithological description, technical parameters, core recovery rate, and RQD variation from Borehole N° 22.

4.2 Industrial requirements

All collected samples were submitted to the Center for Technological Studies and Services in the Construction Materials Industry (CETIM) for the tests and analyses summarized in Table 2.

Table 2. Different analyses performed on gypsum samples

Laboratory work	Number
Sample processing	413
13-element chemical analysis	413
Determination of water of crystallization	413
Chlorine determination	174
X-ray analysis	02

This procedure is designed to determine the qualitative characteristics of the valuable substance. The loss on ignition was measured in accordance with the EN 196-2 standard (Feuerborn, 2011). The crystallization water content was calculated from the weight loss recorded at 400 °C. The chloride concentration was determined potentiometrically, following the requirements of the EN-NF 1744-1 standard. Furthermore, the assessment of gypsum quality complies with the international standard ISO 1587 (1995) and the European standard NF EN 520+A1.Table 3 summarizes the industrial requirements for the manufacturing of construction plaster and its derivatives.

Table 3. Industrial requirements for manufacturing plaster and its derivatives according to ISO 1587 standard

Gypsum category	**Minimum content (100%)**	
	$CaSO_4$ $2H_2O$	**Water for crystallization**
Class - I	Greater than 90%.	More than 18.33
Class - II	80% à 90%	16.74% à 18.83%
Class - III	70% à 80%	14.65% à 16.74%
Class - IV	55% à 70%	11.51% à 14.65%

4.3 Mean values of oxide contents

To determine the elemental composition of the gypsum, a chemical analysis encompassing 13 elements was carried out, and the results are presented in Table 4.

The mean concentration values indicate that CaO and SO_3 are the dominant oxides characterizing the Djebel Djira gypsum (Fig. 9). The results show that the main components of the chemical composition exhibit very similar concentrations, with only negligible variations. These consistent values highlight the homogeneity of the gypsum, which represents the principal stratigraphic layer of the deposit. This observation is further supported by the coefficient of variation ($V < 10\%$), characteristic of elements with highly regular spatial distribution (Smith et al., 2018).

The average contents of CaO, SO_3, and crystallization water (H_2O), measured at 33.46%, 43.58%, and 19.17%, respectively, confirm the good quality of this gypsum. Similar studies have been reported for Messinian gypsum deposits in Tunisie, where CaO and SO_3, ranges between 31–36% and 40–46% (Mahmoudi et al., 2016), confirming the coherence of the Djebel Djira results with other high-quality gypsum occurrences. The levels of potentially deleterious oxides, such as MgO and K_2O, remain within the acceptable chemical thresholds for its use in construction plaster production, in agreement with international standards ASTM C471M, 2016 and EN 13279, 2005. Similarly, the mean chloride content (0.011%) is negligible and consistent with values reported in other exploitable gypsum deposits (Bouzit et al., 2019). The average Na_2O content, determined at 0.09%, shows an irregular distribution across the deposit. Based on these chemical characteristics, the Djebel Djira gypsum can be classified as category I. Histogram analyses reveal a log-normal distribution for SO_3, with tails skewed toward lower values, and a bimodal normal distribution for CaO. Most of the analyzed samples (97%) exhibit CaO concentrations exceeding 30%, while 92% display SO_3 values above 40% and crystallization water contents above 18%, confirming the classification of this material as category I gypsum. The statistical treatment presented here, combining coefficients of variation and frequency distribution analysis, provides a methodological novelty compared to previous studies, which generally focused only on mean chemical values without detailed homogeneity assessment (Lushnikova & Dvorkin, 2016).

Table 4. Chemical composition of Djebel Djira gypsum based on multi-element analysis.

Average chemical composition of the Djebel Djira gypsum deposit						
Variable	**Number**	**Minimum**	**Maximum**	**Average**	**Sigma**	**Variability**
SiO_2	414	0.01	6.25	**0.72**	1.52	209.69
Al_2O_3	414	0.01	1.72	**0.21**	0.44	206.34
Fe_2O_3	414	0.01	0.43	**0.04**	0.17	381.05
CaO	414	30.76	43.16	**33.46**	1.76	5.27
MgO	414	0.01	1.05	**0.30**	0.54	176.57
SO_3	414	37.42	46.00	**43.58**	3.69	8.47
KO_2	414	0.04	0.33	**0.07**	0.09	128.04
NaO_2	414	0.01	0.85	**0.09**	0.26	288.23
TiO_2	414	0.01	0.03	**0.01**	0.005	44.06
P_20_5	414	0.01	0.08	**0.01**	0.02	151.007
LOI	414	21.08	29.29	**21.29**	0.94	4.43
H_2O crystallization	414	16.02	20.69	**19.17**	1.35	7.08
CL	174	0.003	0.053	**0.011**	0.007	62.00

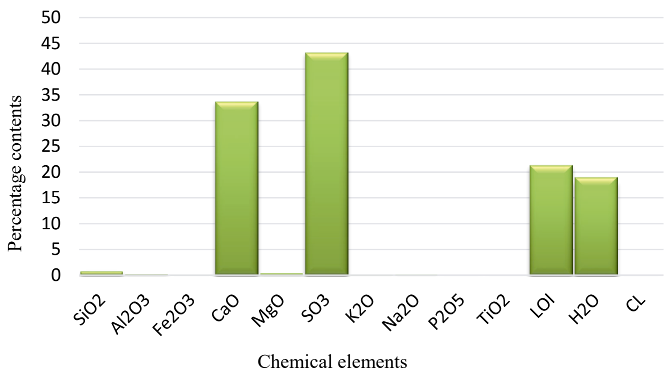

Figure 9. Histogram depicting the mean elemental composition of gypsum from Djebel Djira

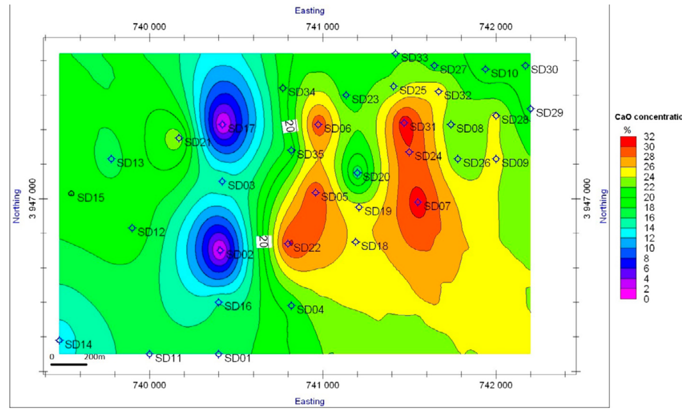

Figure 10. CaO concentration model of the Djebel Djira gypsum deposit.

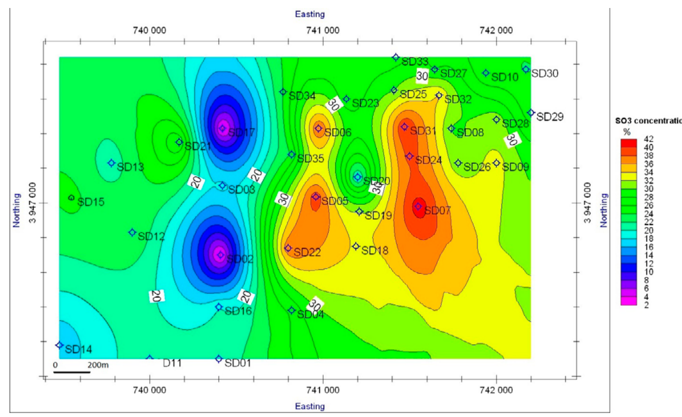

Figure 11. SO_3 concentration variability across the Djebel Djira gypsum deposit.

4.4 X-ray analysis

The X-ray fluorescence (XRF) analysis of two representative gypsum samples reveals a mineralogical composition that is practically identical to that of pure gypsum, with an average purity of 99% (Table 5). Both samples S.7.1P and S.7.2P consist almost exclusively of gypsum, with only trace amounts of dolomite (1%), while calcite and quartz are completely absent. Such results attest to the exceptional purity of the Djebel Djira gypsum, which significantly enhances its suitability for industrial applications, particularly in the production of plaster. Comparable studies on Messinian gypsum deposits of the Fatha Formation (Iraq) have reported slightly lower purities, where accessory minerals such as anhydrite, dolomite, and quartz are more frequently present (Chro & Jamila, 2021). Likewise, Natatou et al., (2012) observed that gypsum deposits in Tahoua region (Niger) commonly contain notable proportions of calcite or silicate impurities, which reduce their overall industrial grade. In this respect, the near-absence of secondary phases in the Djebel Djira gypsum represents a distinctive advantage, ensuring higher chemical stability and lower processing requirements. This outstanding mineralogical homogeneity, combined with the high purity rate, positions Djebel Djira gypsum among the most valuable deposits in the northwestern of Algeria with direct implications for its economic exploitation.

Table 5. Results of X-ray analyses

Sample number	Gypsum	Dolomite	Calcite	Quartz
S.7.1P	99	01	-	-
S.7.2P	99	01	-	-

4.5 Rock quality

Using RockWorks version 17, the quantitative data stored in the project's I-Data table were interpolated into a block (solid) model to generate spatial distribution maps. The results reveal that the CaO concentration within the gypsum deposit exhibits noticeable variability, primarily influenced by compositional heterogeneity and the intercalation of marl and sandstone layers. In particular, the eastern sector of Djebel Djira is characterized by relatively lower CaO contents, ranging between 24% and 32% (Fig. 10). Similar heterogeneities have been reported in Messinian gypsum deposits of the Ebro Basin (Spain), where interbedded marls and siliciclastic inputs also contribute to local variations in CaO content (Orti et al., 2014).

In general, gypsum containing approximately 32.6% CaO is regarded as pure. Within the Djebel Djira deposit, the distribution of SO_3 exhibits a marked spatial variability, with average values reaching about 43.5% in the eastern sector and gradually decreasing to nearly 15% toward the western side (Fig. 11).

A comparative analysis of the two models indicates a gradual replacement of CaO by SO_3 in the eastern and southern sections of the deposit. In contrast, the northern part appears to consist of a formation distinct from limestone or gypsum. The eastern and southern region of the zone may contain a material undergoing transformation into gypsum (Fig. 12).

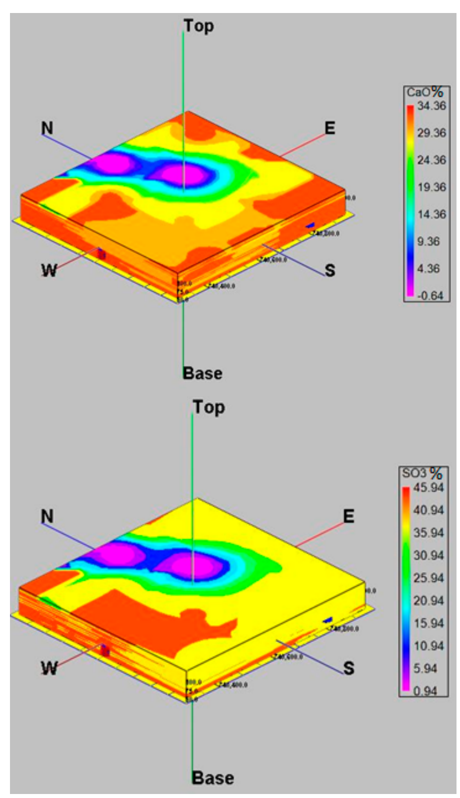

Figure 12. Spatial distribution models of CaO and SO_3 within the Djebel Djira gypsum deposit, generated using RockWorks software.

4.6 Geological reserves

Geological reserves were quantified using the EZ Volume Calculator module of RockWorks 17 software. The Delaunay triangulation method was applied for the volumetric calculation, interconnecting the sampling points in a triangular mesh, with each vertex corresponding to a measurement point. Volumes were determined from the thicknesses (Z values) associated with each triangle, then summed to obtain the total volume. The results indicate an estimated resource of 36 million m³ for gypsum and 26 million m³ for cover layers within the study area, calculated on the basis of an average gypsum thickness of 50 meters.

5. Conclusion

This study provides a comprehensive characterization of the gypsum deposits in the Boufatis Plateau (Lower Chelif Basin, NW Algeria), combining chemical, mineralogical, and geostatistical analyses to assess their industrial potential. Chemical analysis has demonstrated that CaO and SO_3 are the principal oxides characterizing Djebel Djira gypsum. Their consistent distribution, confirms, the homogeneity of the gypsum. The results demonstrate that the Djebel Djira gypsum is of exceptional quality, with average CaO (33.46%) and SO_3 (43.58%) contents compliant with international standards like ISO 1587, and NF EN 520+A1. X-ray diffraction confirmed a purity level of 99%, while low concentrations of deleterious elements such as MgO, K_2O, Na_2O, and chlorides, along with high crystallization water content exceeding 18%, classify it as Category I, ideal for plaster production

Exploiting drilling data with RockWorks and Surfer software revealed spatial heterogeneity. Indeed, the eastern and southeastern sectors exhibit gypsum thicknesses exceeding 50 m with minimal overburden less than 10 m, whereas the western zone, with thicker overburden greater than 40m, is less favorable for extraction. Geotechnical analyses with an average RQD of 65% to 100% indicate good-to-excellent rock mass quality, suitable for stable mining operations.

As a result, Djebel Djira represents a significant natural resource with estimated reserves of 36 million m³. Among the practical recommendations, we propose prioritizing extraction in the East and South-East sectors because the thickness of gypsum exceeds 50 meters, and the cover is less developed. We strongly recommend that thorough environmental impact studies be carried out to ensure sustainable mining of the deposit.

This research addresses major gaps in the understanding of gypsum deposits in Algeria and provides a reproducible methodological framework for resource assessment. Future perspectives should include economic feasibility studies and the development of sustainable extraction protocols, aligned with regional development objectives while preserving natural ecosystems and strictly adhering to environmental standards.

Acknowledgments

The authors sincerely thank the Editor-in-Chief, Prof. Alexander Caneva, for accepting the publication of this article in *Earth Sciences Research*. They are grateful for the opportunity to disseminate their findings to a high-level scientific audience through this journal. Special thanks are extended to the anonymous reviewers for their constructive remarks and valuable expertise, which have significantly improved the quality of this work. The authors also wish to express their deep appreciation to the Knauf Algeria team and the CETIM laboratory for their essential support and assistance.

References

Aloisi, G., Guibourdenche, L., Natalicchio, M., Caruso, A., Haffert, L., El Kilany, A., & Pierre, F. D. (2022). The geochemical riddle of "low-salinity gypsum" deposits. *Geochimica et Cosmochimica Acta,* 327, 247-275. https://doi.org/10.1016/j.gca.2022.03.033

Armatys, M. (2012). *Modification of geomechanical classifications for schistose rock masses.* Ecole Polytechnique, Montreal, Canada.

Atif, K. F. T., Bessedik, M., Belkebir, L., Mansour, B., & Saint Martin, J. P. (2008). Le passage Mio-Pliocène dans le bassin du Bas Chélif (Algérie). Biostratigraphie et paléoenvironnements. *Geodiversitas,* 30(1), 97-116.

Atik, A., Mansouri, M. E. H., Bessedik, M., Osman, M. K., Belkebir, L., Saint Martin, J. P., & Satour, L. (2024). New insights on the latest Messinian-to-Piacenzian stratigraphic series from the Dahra Massif (Lower Chelif Basin, Algeria): Lago Mare, reflooding and bio-events. *BSGF-Earth Sciences Bulletin,* 195(1), 2. https://doi.org/10.1051/bsgf/2023012

Belhadji, A. (2021). *La sédimentation du Miocène supérieur au Pliocène des monts du Dahra (exemples de Djebel Diss et du Plateau d'Ain Merane): aspects litho-stratigraphiques et micropaléontologiques.* Thèse, Université d'Oran, Algérie.

Belhadji, A., Belkebir, L., Saint Martin, J. P., Mansour, B., Bessedik, M., & Conesa, G. (2008). Apports des foraminifères planctoniques à la biostratigraphie du Miocène supérieur et du Pliocène de Djebel Diss (bassin du Chélif, Algérie). *Geodiversitas,* 30 (1), 79-96. DOI: 10.5281/zenodo.5374180. https://doi.org/10.5281/zenodo.5374180

Belkebir, L., Bessedik, M., & Mansour, B. (2002). Le Miocène supérieur du bassin du Bas Chélif: attribution biostratigraphique à partir des foraminifères planctoniques. *Mémoires du Service géologique de l'Algérie,* (11), 187-194.

Belkebir, L., Bessedik, M., Ameur-Chehbeur, A., & Anglada, R. (1996). Le Miocène des bassins nord-occidentaux d'Algérie: Biostratigraphie et eustatisme. *Bulletin des Centres de recherches exploration-production Elf-Aquitaine. Mémoire,* (16), 553-561.

Belkebir, L., Labdi, A., Mansour, B., Bessedik, M., & Saint Martin, J. P. (2008). Biostratigraphie et lithologie des séries serravallo-tortoniennes du massif du Dahra et du bassin du Chélif (Algérie). Implications sur la position de la limite serravallo-tortonienne. *Geodiversitas,* 30(1), 9-19.

Belkebir, L., Mansour, B., Bessedik, M., Saint Martin, J. P., Belarbi, M., & Chaix, C. (1994). Présence d'une construction récifale corallienne à Djebel Chott (Dahra occidentale, Algérie): Témoin du maximum transgressif du Miocène moyen en Méditerranée. *Géologie Méditerranéenne,* 21(1), 1-7. https://doi.org/10.3406/geolm.1994.1492

Benyoucef, M., Bendella, M., Brunetti, M., Ferré, B., Koci, T., Bouchemla, I., & Ghenim, A. F. (2021). Upper Pliocene bivalve shell concentrations from the Lower Chelif basin (NW Algeria): Systematics, sedimentologic and taphonomic framework. *Annales de Paléontologie*, 107, 102509: 1-23. https://doi.org/10.1016/j.annpal.2021.102509

Benzina, M., Hebib, H., & Bensalah, M. (2019). New insights in late Miocene lower Chelif basin biostratigraphy based on planktonic foraminifera (Algeria). *Revue de Micropaléontologie,* 62 (1), 9-24. https://doi.org/10.1016/j.revmic.2018.10.005

Bertoni, C., & Cartwright, J. (2015). Messinian evaporites and fluid flow. *Marine and Petroleum Geology*, 66, 165-176. https://doi.org/10.1016/j.marpetgeo.2015.02.003

Bessedik, M., & Belkebir, L. (1985). Présence du Miocène moyen et supérieur dans la série de la pointe de Canastel (Oran): implications paléoécologiques et biostratigraphiques. *Géologie Méditerranéenne,* 12(3), 147-150. https://doi.org/10.3406/geolm.1985.1344

Bigi, D., Lugli, S., Manzi, V., Roveri, M., Pashko, P., Milushi, I., ... & Lugli, F. (2024). The Messinian salinity crisis onset in Albania: An integrated approach by bio-magnetostratigraphy and rock magnetic analyses. *Palaeogeography, Palaeoclimatology, Palaeoecology,* 638, 112036. https://doi.org/10.1016/j.palaeo.2024.112036

Bleicher, G. (1875). Note sur la geologie des environs d'Oran. *Bulletin de la Société géologique de France,* 1874-1875.

Bouchemla, I., Benyoucef, M., Belhadji, A., Zaidi, M. A., & Chachour, A. (2025). Trace fossil association related to the Upper Miocene transgression cycle in the Lower Chelif Basin, NW Algeria. *Journal of African Earth Sciences,* 222, 105489. https://doi.org/10.1016/j.jafrearsci.2024.105489

Bouzit, S., Laasri, S., Taha, M., Laghzizil, A., Hajjaji, A., Merli, F., & Buratti, C. (2019). Characterization of natural gypsum materials and their composites for building applications. *Applied Sciences,* 9(12), 2443. https://doi.org/10.3390/app9122443

Brives, A. (1897). *Les terrains tertiaires du dassin du Chélif et du Dahra.* Impr. P. Fontana & Company.

Caruso, A., Pierre, C., Blanc-Valleron, M. M., & Rouchy, J. M. (2015). Carbonate deposition and diagenesis in evaporitic environments: The evaporative and sulphur-bearing limestones during the settlement of the Messinian Salinity Crisis in Sicily and Calabria. *Palaeogeography, Palaeoclimatology, Palaeoecology,* 429, 136-162. https://doi.org/10.1016/j.palaeo.2015.03.035

Chalhoub, M. (2006). *Apports des méthodes d'homogénéisation numériques à la classification des massifs rocheux fracturés.* Thèse de doctorat, École Nationale Supérieure des Mines de Paris, France.

Chro, M., & Jamila, J. (2021). Suitability of gypsum from Fatha Formation for production of building materials in Bazian-Takiya area, North-East Iraq. *Tikrit Journal of Pure Science,* 26(3), 53-59. https://doi.org/10.25130/tjps.v26i3.142

Dalloni, M. (1952). *L'atlas tellien occidental.* XIXth International Geological Congress, Algiers, Monographie régionale. 7th series, no 24, Algiers.

Deere, D. U. (1968). Geological considerations. In: K.G. Stagg and O.C. Zienkiewicz (Eds.). *Rock mechanics in engineering practice, Chapter 1*. Wiley, New York. pp. 1–20.

Delfaud, J., Michaux, J., Neurdin, J., & Revert, J. (1973). Un modèle paléogéographique de la bordure méditerranéenne: évolution de la région oranaise (Algérie) au Miocène supérieur. Conséquences stratigraphiques. *Bulletin de la Société d'Histoire naturelle d'Afrique du Nord,* 64, 219-241.

Delteil, J. (1974). *Tectonique de la chaîne alpine en Algérie d'après l'étude du Tell oriental (Monts de la Mina, Beni Chougrane, Dahra).* Thèse de doctorat, Université de Nice, France.

Fenet, B. (1975). *Recherches sur l'alpinisation de la bordure septentrionale du Bouclier africain à partir de l'étude d'un élément de l'orogène nord-maghréb: les monts du Djebel Tessala et les massifs du littoral de l'oranais.* Thèse de doctorat, Université de Nice, France.

Feuerborn, H. J. (2011). *Coal combustion products in Europe-an update on production and utilisation, standardisation and regulation.* World of Coal Ash (WOCA) Conference, Denver, CO, USA.

Gourinard, Y. (1958). *Recherches sur la géologie du littoral oranais. Épirogénèse et nivellements: Par Yves Gourinard.* Service de la carte géologique de l'Algérie.

Guardia, P. (1975). *Géodynamique de la marge alpine du continent africain de l'Oranie Nord-occidentale (Algérie), relation structurale et paléógéographique entre Rif externe et Tell de l'avant pays atlasique.* Thèse de doctorat, Université de Nice, France.

Hebib, H. (2014). *La limite tortono-messénienne dans la marge nord du bassin du bas Chélif. Précisions biostratigraphiques et évolution des assemblages de foraminifères benthiques.* Thèse de doctorat, Université d'Oran 2, Algérie.

Janssens, K. (2004). Chapter 4 X-ray based methods of analysis. *Comprehensive Analytical Chemistry*, 42, 129-226. https://doi.org/10.1016/S0166-526X(04)80008-4

Khalili, R., Satour, L., Mennad, S., & Tadjeddine, H. (2022). Bioérosion et encroûtement sur des huîtres du Pliocène du bassin de Bas Chélif (Algérie nord-occidentale). *Revue de paléobiologie,* 41 (2), 241-265. https://doi.org/10.5281/zenodo.6858361

Krijgsman, W., Rohling, E. J., Palcu, D. V., Raad, F., Amarathunga, U., Flecker, R., ... & Aloisi, G. (2024). Causes and consequences of the Messinian salinity crisis. *Nature Reviews Earth & Environment,* 5(5), 335-350. https://doi.org/10.1038/s43017-024-00533-1

Lanzoni, A. (2022). *The Messinian Salinity Crisis in the Adriatic Sea*. Theses, Università Degli Studi di Trieste. Italy

Lushnikova, N., & Dvorkin, L. (2016). Sustainability of gypsum products as a construction material. *Sustainability of Construction Materials (Second Edition),* 643-681. https://doi.org/10.1016/B978-0-08-100370-1.00025-1

Mahmoudi, S., Bennour, A., Chalwati, Y., Souidi, K., Thabet, M., Srasra, E., & Zargouni, F. (2016). Tunisian gypsums: Characteristics and use in cement. *Journal of African Earth Sciences,* 121, 267-273. https://doi.org/10.1016/j.jafrearsci.2016.05.023

Mansouri, M. E. H., Bessedik, M., Aubry, M. P., Belkebir, L., Mansour, B., & Beaufort, L. (2008). Contributions biostratigraphiques et paléoenvironnementales de l'étude des nannofossiles calcaires des dépôts tortono-messiniens du bassin du Chélif (Algérie). *Geodiversitas,* 30 (1), 59-77.

McQuillan, A., & Bar, N. (2023). The necessity of 3D analysis for open-pit rock slope stability studies: Theory and practice. *Journal of the Southern African Institute of Mining and Metallurgy,* 123 (2), 63-70.

Moulana, M. L., Hubert, A., Guendouz, M., El Ouahabi, M., Boutaleb, A., & Boulvain, F. (2021). Contribution to the sedimentology of the Messinian carbonates of the Chelif Basin (Boukadir, Algeria). *Geologica Belgica,* 24 (1-2). https://doi.org/10.20341/gb.2021.002

Moussa, K., Belkebir, L., Mansour, B., & Bessedik, M. (1994). Dynamique et évolution de la Marge Sud du Bassin du Chelif (Algérie) vers une plate-forme carbonatée (Miocène supérieur). Approche sédimentologique et stratigraphie séquentielle. *Géologie Méditerranéenne,* 21(3), 131-132. https://doi.org/10.3406/geolm.1994.1545

Natatou, I., Marou, G., Adamou, Z., Moussa, Y., & Boos, A. (2012). Caractérisation physico-chimique du gypse de Tahoua. *International Journal of Biological and Chemical Sciences*, 6(3), 1324-1336. DOI: 10.4314/ijbcs.v6i3.35

Neurdin-Trescartes, J. (1992). *Le remplissage sédimentaire du bassin néogène du Chélif, modèle de référence de bassins intramontagneux.* Thèse de doctorat, Université de Pau et Pays de l'Adour.

Neurdin-Trescartes, J. (1995). Palaeogeographie du Bassin du Chélif (Algérie) au Miocène. Causes et conséquences. *Géologie Méditerranéenne,* 22(2), 61-71. https://doi.org/10.3406/geolm.1995.1569

Ortí, F., Rosell, L., Gibert, L., Moragas, M., Playà, E., Inglès, M., Rouchy, J. M., Calvo, J. P., & Gimeno, D. (2014). Evaporite sedimentation in a tectonically active basin: The lacustrine Las Minas Gypsum unit (Late Tortonian, SE Spain). *Sedimentary Geology*, 311, 17-42. https://doi.org/10.1016/j.sedgeo.2014.06.004

Pérez-Asensio, J. N., Aguirre, J., Jiménez-Moreno, G., Schmiedl, G., & Civis, J. (2013). Glacioeustatic control on the origin and cessation of the Messinian salinity crisis. *Global and Planetary Change,* 111, 1-8. https://doi.org/10.1016/j.gloplacha.2013.08.008

Perrodon, A. (1957). Etude géologique des bassins néogènes sublittoraux de l'Algérie occidentale. *Publication du Service de la Carte géologique d'Algérie*, 12, 1-323.

Pomel, A. (1892). Sur la classification des terrains miocènes de l'Algérie et réponses aux critiques de M. Peron. *Bulletin de la Société géologique de France,* 166-174.

Remmache, I. (2006). *Potentiel en substances utiles non métalliques (gypse et sel gemme) du bassin de Mila (Algérie nord orientale)*. Thèse Magister, Université Mentouri, Constantine, Algérie, 95p.

Repal, S. N. (1952). Le bassin néogène du Chélif. XIXe Congr. Inter. Geol, Monogra. Région (Algérie), 1, 16, 56p.

Repelin, J. (1895). *Étude géologique des environs d'Orléansville.* Barthelet, 202 pages

Rouchy, J. M. (1982). La genèse des évaporites messiniennes de Méditerranée. *Paris: Éditions du Muséum national d'Histoire naturelle,* 50(1-267).

Rouchy, J. M., & Monty, C. L. (1981). Stromatolites and cryptalgal laminites associated with Messinian gypsum of Cyprus. In: Monty, C. (Eds). *Phanerozoic Stromatolites*. Springer, Berlin, Heidelberg. https://doi.org/10.1007/978-3-642-67913-1_13

Rouchy, J. M., Caruso, A., Pierre, C., Blanc-Valleron, M., & Bassetti, M. A. (2007). The end of the Messinian salinity crisis: Evidences from the Chelif Basin (Algeria). *Palaeogeography, Palaeoclimatology, Palaeoecology,* 254(3-4), 386-417. https://doi.org/10.1016/j.palaeo.2007.06.015

Roveri, M., Flecker, R., Krijgsman, W., Lofi, J., Lugli, S., Manzi, V., Sierro, F. J., Bertini, A., Camerlenghi, A., De Lange, G., Govers, R., Hilgen, F. J., Hübscher, C., Meijer, P. T., & Stoica, M. (2014). The Messinian Salinity Crisis: Past and future of a great challenge for marine sciences. *Marine Geology,* 352, 25-58. https://doi.org/10.1016/j.margeo.2014.02.002

Saint-Martin, J. P. (1987). *Les formations récifales coralliennes du Miocène supérieur d'Algérie et du Maroc. Aspects paléoécologiques et paléogéographiques.* Thèse de doctorat, Université, d' Aix Marseille, France.

Saint-Martin, J. P., & André, J. P. (1992). Les constructions coralliennes de la plate-forme carbonatée messinienne de Malte. *Géologie Méditerranéenne*, 19(3), 145-163. https://doi.org/10.3406/geolm.1992.1474

Satour L., Lauriat-Rage, A., Belkebir, L., & Bessedik, M. (2013). Biodiversity and taphonomy of bivalves assemblages of the Pliocene of Algeria (Bas Chelif basin). *Arabian journal of Geosciences,* 7, 5295-5308. https://doi.org/10.1007/s12517-013-1154-4

Sellam, Y., Gruchola, S., Tulej, M., Keresztes-Schmidt, P., Riedo, A., Meddane, S., & Wurz, P. (2025). The search for ancient life on Mars using morphological and mass spectrometric analysis: an analog study in detecting microfossils in Messinian gypsum. *Frontiers in Astronomy and Space Sciences,* 12:1503042. https://doi.org/10.3389/fspas.2025.1503042

Shen, W., Ni, W., Yong, R., Huang, L., Ye, J., Luo, Z., & Du, S. (2023). Estimating RQD for Rock Masses Based on a Comprehensive Approach. *Applied Sciences,* 13(23), 12855. https://doi.org/10.3390/app132312855

Smith, G. L., & Brooks, L. (2018). Incorporation of the socio-cultural dimension into strategic long-term planning of mineral assets in South Africa. *Journal of the Southern African Institute of Mining and Metallurgy,* 118(4), 331–336. https://doi.org/10.17159/2411-9717/2018/v118n4a1

Stefano, L., Vinicio, M., Marco, R., & Charlotte, S. B. (2010). The Primary Lower Gypsum in the Mediterranean: A new facies interpretation for the first stage of the Messinian salinity crisis. *Palaeogeography, Palaeoclimatology, Palaeoecology,* 297 (1), 83-99. https://dx.doi.org/10.1016/j.palaeo.2010.07.017

Thomas, G. (1985). *Géodynamique d'un bassin intramontagneux: Le Bassin du Bas-Chelif occidental (Algérie) durant le mio-plio-quaternaire.* Thèse de doctorat, Université de Pau et Pays de l'Adour, France.

Yu, X., He, M., Hao, W., & Wang, H. (2024). Drilling Process Monitoring for Predicting Mechanical Properties of Jointed Rock Mass: A Review. *Buildings, 14*(7), 1992. https://doi.org/10.3390/buildings14071992

Zheng, Y., Chen, C., Liu, T., Song, D., & Meng, F. (2023). Mechanical properties and fracturing behavior of jointed rock mass under uniaxial compression: insights from numerical simulations. *Scientific Reports*, 13, 1463.